DOI: 10.13009/EUCASS2017-148

A numerical mesoscale model for aluminum agglomeration in solid propellants

Mathieu PLAUD and Stany GALLIER***
Airbus Safran Launchers, 91710 Vert-le-Petit, France
**mathieu.plaud@airbusafran-launchers.com*
***stany.gallier@airbussafran-launchers.com*

Abstract

The formation of aluminum agglomerates during combustion of aluminized solid propellants is known to have a significant impact on the behavior of the motor. In this paper, we propose a phenomenological agglomeration model whose input data is obtained from a mesoscale solid propellant simulation code. This new coupling strategy is very promising since it has the potential to model various physical effects on agglomeration. First applications of the model on a typical industrial propellant show encouraging agglomerate size distributions consistent with classical experimental data.

1. Introduction

Aluminized solid propellants are widely used for industrial solid rockets. However, it is well-known that agglomeration of aluminum is likely to occur: particles may coalesce at the propellant burning surface resulting in the ejection in the flow of agglomerates much bigger than the initial virgin aluminum. Agglomeration can be critical from both a performance and stability standpoint. Associated two-phase losses, slag accumulation, nozzle erosion or incomplete combustion do indeed burden the expected theoretical thrust. Pressure oscillations are also known to be affected by the presence of aluminum distributed combustion in the chamber. Therefore much effort has been made through past years to experimentally characterize agglomeration and to understand the underlying physics that drives the phenomenon. However in spite of a considerable amount of work, some aspects of the agglomeration process still remain poorly understood. An illustration of the involved complexity is the given by review of Price et al [1] where agglomeration is shown to be dependent on various parameters such as propellant composition, aluminum initial size distribution or chamber pressure. A consequence of this defying complexity is that it remains merely impossible to make accurate ab initio estimations of agglomeration. Then, large and costly experiments are often mandatory to get a grasp on the agglomeration behavior.

In this context, modeling strategies can be very valuable by yielding an estimation of the size of aluminum agglomerates. Given the complicated physics involved, models used industrially are often very simple, mainly resting on empirical or geometrical considerations. A first category of models are empirical models based on the compilation of numerous experimental data from which trends and correlations are extracted which link a mean agglomerate size to various parameters (oxidizer fraction, combustion rate, …). One can cite the widespread correlations of Salita [2] and Beckstead [3]. These models naturally lack predictability when used to study agglomeration in new propellant compositions and give no information about the physics involved in the process. A second modeling category is referred to as pocket models [4-5]. In these approaches, relevant geometrical information about the propellant is first extracted (e.g. free volume between coarse oxidizer particles) in order to build “pockets” which are zones in which aluminum particles will concentrate. All the aluminum encapsulated in these pockets is supposed to coalesce to form a final single agglomerate. A simple relation between propellant properties (coarse oxidizer size and mass loading) and agglomerate size is finally obtained. Even if these simple approaches generally give correct orders of magnitude they are often not sufficient. For example, no dependence on the original aluminum size or the operating pressure is considered while these are known to have a significant effect on agglomeration. They also fail to give relevant results for propellant containing non monomodal oxidizer. A third category of models are stochastic microstructure models. They are based on a microstructure reconstruction of the studied propellant (random pack) [6-7]. Gallier [8] and Bandera et al [9] developed predictive agglomeration models which yield correct agglomerate size but only under the form of a mass averaged D_{43} diameter instead of a size distribution. In the same spirit, Jackson [10] proposed an approach based on a proximity criterion of aluminum particles in a random pack. This model returns an agglomerate size distribution but is very dependent on the threshold value used in the criterion. From their geometrical nature, these models cannot take into account the influence of pressure nor the dependency on the oxidizer type.

DOI: 10.13009/EUCASS2017-148

The approach we consider in this paper belongs to a last category of phenomenological models. These models aim at describing the agglomeration process by explicitly following the evolving position of the initial aluminum particles and their interaction with the surrounding solid and gas phases. Various different phenomenological models have already been developed [11-17]. They differ from the agglomeration mechanisms that are considered and the level of details that is given to the description of the propellant surface and gas phase. For example one can mention the works of Rashkovskii [17] where the agglomeration formation model is based on a force balance that applies to an aggregate (group of sintered aluminum particles, also referred to as accumulate in the literature) standing at the propellant surface. As a result of the stresses and torques that apply to the aggregate, the mobility of the latter at the surface can be considered. If the aerodynamic forces exceed the adhesion force retaining the aggregate at the surface, the latter is ejected and supposed to melt in the gas flow. In this approach, temperature does not play any role in the agglomerate formation mechanism. On the opposite, Sambamurthi et al [12] consider a formation mechanism based solely on temperature: an aggregate at the surface will eventually reach a high enough temperature for its melting and subsequent ejection to occur. In their approach, regression of the burning front is taken into account in a simplistic way where no deformation of the front is considered. The two aforementioned models are able to yield size distribution of the agglomerate size and take into account the effects of pressure and initial size distribution. However the mechanisms considered are quite different. Our approach tries to incorporate both formation mechanisms as well as a better description of the surface topology thanks to a weak coupling with a mesoscale combustion code.

The paper is organized as follows. In a first part we describe the mechanisms that are considered for the formation of both aluminum aggregates and agglomerates. In a second part we introduce the agglomeration model from a numerical perspective. In a third part we briefly describe the mesoscale combustion code that is used to provide input data and the coupling with the agglomeration model. Finally, we show preliminary results obtained with our methodology.

2. Agglomeration mechanisms for composite propellants

In this work we focus on the study of agglomeration for composite solid propellants. For this kind of propellants, even though uncertainties remain, the following global agglomeration mechanism is retained in our approach, taken from the experimental observations of [1]. First, aluminum particles initially present in the solid phase are progressively heated with the advance of the burning front. Possible sintering of these particles can occur in solid phase due to dilatation. In a second step, aluminum particles (passivated by a thin nanometric alumina layer) emerge at the surface, composed of a binder decomposition liquid layer and/or solid carbonaceous residues. They are retained for some time at the surface due to still poorly-understood adhesion processes (capillarity, hydrodynamic forces, carbonaceous residues trapping ...) and reach temperature higher than aluminum melting point. In a third step, contacting particles cluster under the form of aggregates. The physical sintering mechanism at the surface remains unclear but the following two-step mechanism is proposed in [1]: particles are first connected either by solid phase sintering or carbon residues bridges. Then, with increasing temperature, the external alumina layer cracks and liquid aluminum leaking out of the shell generates alumina bridges between particles when placed in an oxidizing atmosphere. Due to aerodynamic forces, mobility can occur at the surface of the propellant, possibly enhancing contacts between neighboring aggregates. Finally, two kinds of events can occur at this stage: 1) the aggregate leaves the surface when aerodynamic forces exceed adhesion forces or 2) the aggregate reaches alumina melting temperature (approximately 2300K) and the aluminum particles coalesce causing the ejection into the flow.

3. Coupling methodology

Based on the phenomenology described above, we develop a numerical model for agglomeration in composite solid propellants. Even though the proposed methodology is general, we will in a first time focus on the study of classical aluminized AP (Ammonium Perchlorate)-HTPB (hydroxyl-terminated polybutadiene) propellants. We discuss hereafter the global outline of our approach. Like the other existing phenomenological models, the starting point of our approach is the construction of a random pack which is representative of the propellant microstructure. These packs contain both AP and aluminum particles (see Figure 1).

DOI: 10.13009/EUCASS2017-148

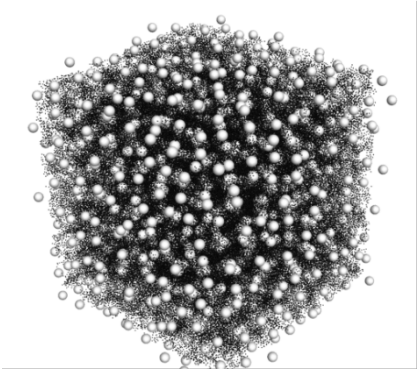

Figure 1: Representative microstructure. Random pack with coarse AP (white) and aluminum (black) particles.

The combustion of the propellant is then explicitly solved by a dedicated code (Section 4) to obtain information that is used as input for our agglomeration model (Section 5). Neither agglomeration nor combustion of aluminum particles is considered in the propellant combustion simulations. The proposed approach should therefore be viewed as a weak coupling methodology where the combustion code is used to provide a good approximation of the surface topology and temperature and velocity fields near the burning front.

4. Mesoscale combustion code

4.1 Governing equations

We give hereafter a brief overview of the mesoscale combustion code that is used to provide the input data of our agglomeration model. Both solid and gas phase are considered and coupling between the two phases is taken into account by enforcing proper jump conditions. In the solid phase, we simply solve for the heat equation:

$$\rho_c C_c \frac{\partial T}{\partial t} = \nabla . \lambda_c \nabla T \quad \textbf{(1)}$$

where T is the temperature and ρ_c, C_c, λ_c respectively designate the density, heat capacity and thermal conductivity of the condensed phase. Note that thermochemical variables vary in space depending on whether a cell is located in the binder or in AP. In the gas phase, the unity Lewis number Low-Mach Navier-Stokes equations are considered:

$$\frac{\partial \rho_g}{\partial t} + \nabla . \rho_g \boldsymbol{U} = 0 \quad \textbf{(2)}$$

$$\frac{\partial \boldsymbol{U}}{\partial t} + \boldsymbol{U} . \nabla \boldsymbol{U} = -\frac{\nabla p}{\rho_g} + \frac{1}{\rho_g} \nabla . \mu \nabla \boldsymbol{U} \quad \textbf{(3)}$$

$$\frac{\partial T}{\partial t} + \boldsymbol{U} . \nabla T = \frac{1}{\rho_g C_g} \nabla . \lambda_g \nabla T + \frac{\dot{\omega}_T}{\rho_g C_g} \quad \textbf{(4)}$$

$$\frac{\partial Y_k}{\partial t} + \boldsymbol{U} . \nabla Y_k = \frac{1}{\rho_g} \nabla . \frac{\lambda_g}{C_g} \nabla Y_k + \frac{\dot{\omega}_k}{\rho_g} \quad \textbf{(5)}$$

$$\rho_g = \frac{P_0 W}{RT} \quad \textbf{(6)}$$

with $\boldsymbol{U} = (u, v, w)$ the fluid velocity vector, p the hydrodynamic pressure, μ the viscosity, W the molecular weight and P_0 the thermodynamic (constant) pressure. Coupling between the two phases is assured by enforcing the following jump conditions at the surface:

$$[\rho(\boldsymbol{U} . \boldsymbol{n} + r_b)] = 0 \quad \textbf{(7)}$$

$$\left[\frac{\lambda}{C} \nabla Y_k . \boldsymbol{n}\right] = \dot{m}[Y_k] \quad \textbf{(8)}$$

$$[\lambda \nabla T . \boldsymbol{n}] = -\dot{m} Q_s + \varphi \quad \textbf{(9)}$$

with $[.] \equiv (.)_g - (.)_s$ and $\boldsymbol{n}$ is the normal vector to the surface (oriented toward the gas). The heat of decomposition Q_s models the reactions taking place at the surface and the additional heat flux φ can be used to model either a transient ignition flux or an external radiative flux coming from the combustion of aluminum. A global chemistry modeling inspired from the well-known BDP model [18] is considered in the gas phase to model the complex chemical reactions. The BDP model is known to give a correct estimation of the complex flame structure in the gas

DOI: 10.13009/EUCASS2017-148

flame for AP/HTPB propellants and is thus well-suited here since gas temperature profiles will be used as input in the agglomeration model. Regression rate of the front is given by an Arrhenius law:

$$r_b = A_s e^{-E_s/RT_s} \quad \textbf{(10)}$$

where T_s is the surface temperature and the parameters of the law once again depend on whether a point at the surface is located in the binder or in AP. The unsteady position of the front is tracked using a Level-Set function Ψ which satisfies the following Hamilton-Jacobi equation:

$$\frac{\partial \psi}{\partial t} + r_b \|\nabla \psi\| = 0 \quad \textbf{(11)}$$

Numerical procedure and more details about the code can be found in [19].

4.2 Input data for the agglomeration model

As already mentioned, the agglomeration model takes as input a random pack containing the position and size of the aluminum particles. During the combustion simulation, other relevant information is collected and periodically saved. Each save file corresponds to a given physical time and stores the following data: position of the front (coordinates of nodes located at the surface), velocity field of injected gases, solid composition of the surface (whether a node is located in the binder or in AP), temperature profile in the gas phase and surface temperature. Note that saving frequency should note be too low in order for transient phenomena to be properly captured by the agglomeration model.

5. Agglomeration model

5.1 Initial set-up and time evolution

The set-up of the model consists in reading the position and radius of aluminum particles in the random pack file. The first combustion save file is also read at this stage. In particular we know the initial position of the burning front. Given this information we split the domain into three parts: the non-decomposed solid propellant (referred to as “solid phase”), a surface layer composed of binder decomposition products and the gas phase. The agglomeration model proceeds in an unsteady fashion. After the initial set-up, time is advanced with a time step estimated from the maximum burning rate at the surface and the minimum aluminum particle size:

$$\Delta t = \frac{1}{\beta} \frac{\min(D)}{\max(r_b)} \quad \textbf{(12)}$$

where a typical value of parameter β is 20. For time $t^n = n\Delta t$, relevant input data (gas velocity, gas temperature …) is linearly interpolated from the results saved during the combustion simulation. Then the following steps are sequentially performed: particle tracking and aggregate formation, detection of contact between aggregates, evaluation of aggregate surface mobility and finally, formation of agglomerates. Each step will be detailed in the following sections.

5.2 Particle tracking and aggregate formation

At the beginning of the agglomeration simulation, all the aluminum particles belong to the solid phase. As the front recesses, a particle will completely leave the solid phase, entering the surface layer. According to the physical mechanisms detailed in Section 2, particles are supposed to be retained at the surface and will consequently follow the displacement of the burning front. With time they are likely to collide with other particles located in the solid phase resulting in the formation of aluminum aggregates (Figure 2).

DOI: 10.13009/EUCASS2017-148

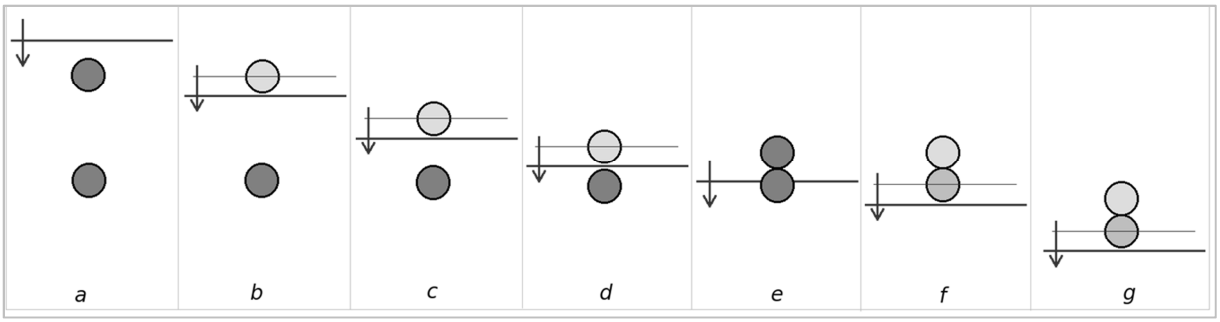

Figure 2: Aggregate formation process for two aluminum particles initially belonging to the solid phase (a). The first encountered particle leaves the solid phase and is trapped by the surface layer (b) and follows the burning front (c). It collides with the second particle (d) generating an aggregate (e) that does not move until the second particle in turn leaves the solid phase (f).

During this "regression stage", all particles belonging to a given aggregate move at the same speed equal to the velocity of the last added “pilot” particle. As will be seen later, when the pilot particle does not intersect the solid phase, an aggregate is free to move at the surface: we refer to these displacements as *aggregate mobility*. As a consequence, when evaluating the aggregate formation process, we must also check for any contact between two neighboring aggregates. In the eventuality of contact, the two aggregates are merged. This mobility, confirmed by experimental visualization, can play a role on the final size of the agglomerates and should be taken into account.

5.3 Evaluation of aggregate mobility

Evaluating the forces acting on an aggregate enables us to determine if it will be ejected away from the surface into the gas flow or remain at the surface, retained by adhesion forces. In the latter case, we can compute the aforementioned aggregate mobility. If the pilot particle of an aggregate belongs to the solid phase then no displacement or ejection is possible. Otherwise, our model authorizes an aggregate to move both by translation, tangentially to the surface, and rotation around the “pilot” particle. This displacement is computed by solving a simplified problem. First we describe the aggregate as an equivalent spheroid (Figure 3) of semi-axes a and b ($a<b$).

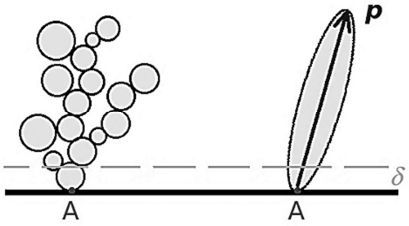

Figure 3: Spheroid equivalent (right) to the aggregate (left)

Point A designates the contact point between the surface and the aggregate. An equivalent geometry is built via a vector $\boldsymbol{p}$ associated to each moving aggregate whose direction is obtained by: $\boldsymbol{p} \propto \sum \boldsymbol{AM_i}$ with $\boldsymbol{M_i}$the center of particles belonging to the aggregate and whose norm is given by $\|\boldsymbol{p}\| = 2\|\boldsymbol{AG}\|$ where G is the center of mass of the aggregate.

We detail the different forces considered in the model. First, since the aggregate is located in a gas flow, we take into account a drag-induced aerodynamic force whose expression depends on the shape of the ellipsoid. In the case of an elongated shape ($\varepsilon = a/b \ll 1$) the force expression is approximated by the Slender Body Theory in a Stokes regime:

$$\boldsymbol{F_{h_i}} = 6\widetilde{\mu_g}\pi b\left[X^A \boldsymbol{p}_i\boldsymbol{p}_i + Y^A\left(\delta_{ij} - \boldsymbol{p}_i\boldsymbol{p}_i\right)\right]\left(\overline{\boldsymbol{U}}_{j-}\boldsymbol{U}^{\boldsymbol{p}}{}_j\right) \quad \textbf{(13)}$$

$$X^A = \frac{4E}{6-3E} \qquad Y^A = \frac{8E}{6+3E} \quad \textbf{(14)}$$

$$E = \frac{1}{\ln(2/\varepsilon)} \text{ with } \varepsilon = a/b \quad \textbf{(15)}$$

DOI: 10.13009/EUCASS2017-148

where $\widetilde{\mu_g}$ is the gas viscosity, δ_{ij} the Kronecker symbol and $(\bar{\boldsymbol{U}} - \boldsymbol{U^p})$ the difference between the gas velocity $\bar{\boldsymbol{U}}$, extracted from combustion simulation, and the aggregate velocity $\boldsymbol{U^p}$. If the parameter ε does not take a small value then the aggregate is simply modeled as an equivalent sphere and the acting force reads:

$$\boldsymbol{F_{h_i}} = 6\widetilde{\mu_g}\pi b\delta_{ij}\left(\bar{\boldsymbol{U}}_j - \boldsymbol{U^p}_j\right) \tag{16}$$

Aerodynamic forces tend to move the aggregate away from its initial position. They can be written under the general form: $\boldsymbol{F_h} = \bar{\bar{\boldsymbol{\alpha}}}_{\boldsymbol{h}}(\bar{\boldsymbol{U}} - \boldsymbol{U^p})$. On the opposite, two kinds of adhesion forces that restrain the movement are inserted into the model. First a force oriented normal to the surface whose intensity depends on the number of particles located in the liquid/carbon residues layer, noted Ω_δ, at the surface is considered. The maximum value of this force, which has to be exceeded to cause ejection, is given by:

$$\boldsymbol{F_a}^{\boldsymbol{max}} = \left(\sum_{k\in\Omega_\delta} \delta\,\widetilde{k_a}\right)\boldsymbol{n} \tag{17}$$

with $\widetilde{k_a}$ a parameter whose value depends on the composition of the liquid layer. The width of this liquid layer δ is obtained for the binder by:

$$\delta \cong \frac{\alpha}{r_b}\ln\left(\frac{T_s - T_0}{T_f - T_0}\right) \tag{18}$$

where α is the thermal diffusivity, r_b the local burning rate, T_s the local surface temperature, T_0 the initial temperature and T_f the binder melting temperature (~550K). The second adhesion force in the model is a viscous force tangent to the surface. Its expression corresponds to the drag force applying on a macro-particle of diameter δ and intends to represent how the high-viscosity molten binder impedes aggregate motion.

$$\boldsymbol{F_{v_i}} = 3\widetilde{\mu_l}\pi\delta\delta_{ij}\left(\boldsymbol{0} - \boldsymbol{U^p}_j\right) \tag{19}$$

Once again, this force can be written under the general form: $\boldsymbol{F_h} = \bar{\bar{\boldsymbol{\alpha}}}_{\boldsymbol{v}}(\boldsymbol{0} - \boldsymbol{U^p})$. Figure 4 illustrates the different forces that act on the aggregate:

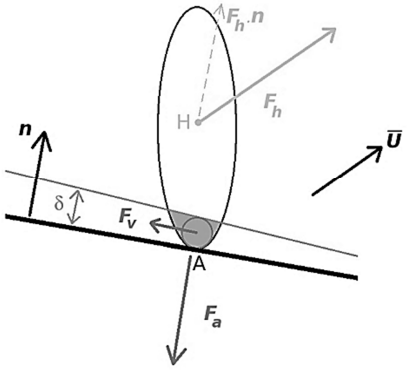

Figure 4: Forces acting on a moving aggregate

Once these forces have been defined we proceed in two steps. First we evaluate the following criterion which indicates whether the aggregate will leave the surface due to overwhelming aerodynamic forces:

$$(\bar{\bar{\boldsymbol{\alpha}}}_{\boldsymbol{h}}\bar{\boldsymbol{U}} - \boldsymbol{F_a}^{\boldsymbol{max}}).\boldsymbol{n} > 0 \tag{20}$$

The criterion not being fulfilled means that adhesion forces will maintain the aggregate at the surface. The equilibrium of forces is then verified for:

$$\boldsymbol{F_a} = -[\bar{\bar{\boldsymbol{\alpha}}}_{\boldsymbol{h}}\bar{\boldsymbol{U}}.\boldsymbol{n}].\boldsymbol{n} \tag{21}$$

Once all acting force has received a value the second step consists in solving the classical Newton-Euler equations to compute the motion of aggregates:

DOI: 10.13009/EUCASS2017-148

$$m\frac{d\boldsymbol{U^p}}{dt} = \boldsymbol{F_h} + \boldsymbol{F_v} + \boldsymbol{F_a} \quad \textbf{(22)}$$

$$J_{/A}\frac{d\boldsymbol{\Omega_{/A}}}{dt} = \boldsymbol{AH} \wedge \boldsymbol{F_h} \quad \textbf{(23)}$$

First-order implicit integration in time of the above system leads to:

$$m\frac{(\boldsymbol{U^{p^{n+1}}} - \boldsymbol{U^{p^n}})}{\Delta t} = \bar{\bar{\boldsymbol{\alpha}}}_{\boldsymbol{h}}(\bar{\boldsymbol{U}} - \boldsymbol{U^{p^{n+1}}}) + \bar{\bar{\boldsymbol{\alpha}}}_{\boldsymbol{v}}(\boldsymbol{0} - \boldsymbol{U^{p^{n+1}}}) + \boldsymbol{F_a} \quad \textbf{(24)}$$

$$J_{/A}\frac{(\boldsymbol{\Omega_{/A}}^{n+1} - \boldsymbol{\Omega_{/A}}^{n})}{\Delta t} = \boldsymbol{AH} \wedge \bar{\bar{\boldsymbol{\alpha}}}_{\boldsymbol{h}}(\bar{\boldsymbol{U}} - \boldsymbol{U^{p^{n+1}}}) \quad \textbf{(25)}$$

The position of each of the particle belonging to the aggregate is then updated thanks to the translation and rotation computed velocities:

$$\boldsymbol{X_i}^{n+1} = \boldsymbol{X_i}^{n} + \Delta t(\boldsymbol{U^{p^{n+1}}} + \boldsymbol{\Omega_{/A}}^{n+1} \wedge \boldsymbol{AM_i}) \quad \textbf{(26)}$$

In all the above equations, the $\widetilde{(.)}$ notation tags the model free parameters which can be adjusted to transcribe proper mobility/ejection behavior. These parameters mainly alter the behavior of the model regarding aggregate mobility and amplitude of adhesion forces.

5.4 Formation of aluminum agglomerates

In our approach, aluminum agglomerates can form in two ways. First, an aggregate can be ejected into the flow due to aerodynamic forces exceeding adhesion forces. The associated particles will eventually coalesce far from the surface to give the agglomerate. This first formation mode is already taken care of by the problem solved in the previous section.

In the second formation mode, aluminum particles composing the aggregate reach the alumina melting temperature T_{f,Al_2O_3}(~2300K) while still being at the surface: liquid aluminum particles then promptly coalesce due to surface tension into an agglomerate that consequently leaves the surface. In order to keep the whole model computationally tractable we chose here to make a simple assumption: if one of the particles of the aggregate enters the zone where gas temperature exceeds T_{f,Al_2O_3} then coalescence is supposed to occur immediately. Even if the approach is simplistic it is expected to yield relevant results. Indeed, if we compare the characteristic particle displacement time $\tau_v = D/r_b$ and a thermal characteristic time $\tau_T = D^2/\alpha_{Al}$ we observe that for common values of initial aluminum size (D~10µm) and propellant burning rate (r_b~10mm/s) the ratio τ_T/τ_v is very small (~10^{-3}). This statement legitimates the above assumption. Note that this simple approach is also interesting from a numerical perspective since we only need to store the iso-profile T=2300K instead of the whole gas temperature field.

6. Preliminary results

The proposed methodology is applied to a typical industrial propellant loaded with 68% 200µm AP and 18% 20µm Al mass fraction. We focus here on qualitative agglomeration trends and comparison with classical approaches like correlations and pocket models on this simple case. The detailed study of the effect of the model free parameters or quantitative comparison with experimental results will be addressed in further study.

First a random pack is generated (Figure 1) and a mesoscale combustion simulation conducted to provide input data for the agglomeration model. A typical output of our combustion code is illustrated in Figure 5 where the recessing burning front is colored by surface temperature. One can clearly observe that surface is non-planar due to both the heterogeneous temperature field and space-dependent pyrolysis laws.

DOI: 10.13009/EUCASS2017-148

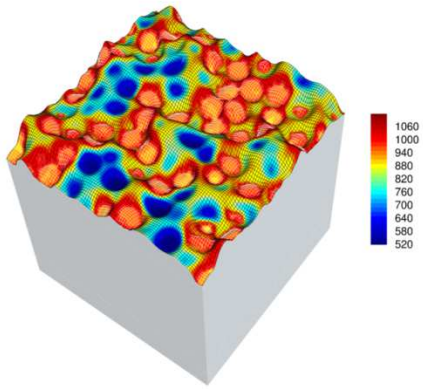

Figure 5: Surface temperature field on the burning front. White mesh cells represent AP and black mesh cells HTPB.

The agglomeration model is then applied to determine the agglomerate size distribution. In the present simulation, we make the following assumptions: aggregates are ejected in the flow as soon as the underlying surface is made of AP particles ($\widetilde{k_a}(AP) = 0$ in Eqn.17). On the opposite no aerodynamic ejection is supposed to occur if the pilot particle is located in the binder ($\widetilde{k_a}(HTPB) = \infty$). Surface mobility is not considered ($\widetilde{\mu_g} = 0$, $\widetilde{\mu_l} = \infty$). Figure 6 gives a representation of the results of our model with aggregates forming at the surface and coalesced agglomerates ejected and carried away from the surface by the gas flow.

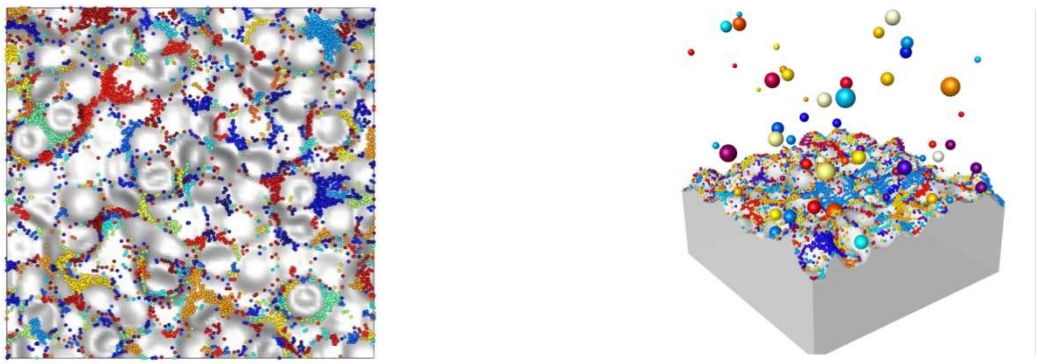

Figure 6: Results of the agglomeration model. Left: Top view with surface aggregates only. Right: Perspective with surface aggregates and ejected agglomerates.

In the above figures particles are colored by the aggregate they belong to. One can see that large aggregates form in "cold" zones located between coarse AP particles. These zones appear clearly in Figure 5. These aggregates are ejected in the flow when a primary flame or Leading-Edge Flame (LEF) [20] forms above the surface at the junction between AP and HTPB. At this location the 2300K iso-surface is very close to the surface and aggregate coalescence is highly probable. All generated agglomerates (~10 000) are numerically collected and the obtained size distribution is plotted in Figure 7.

DOI: 10.13009/EUCASS2017-148

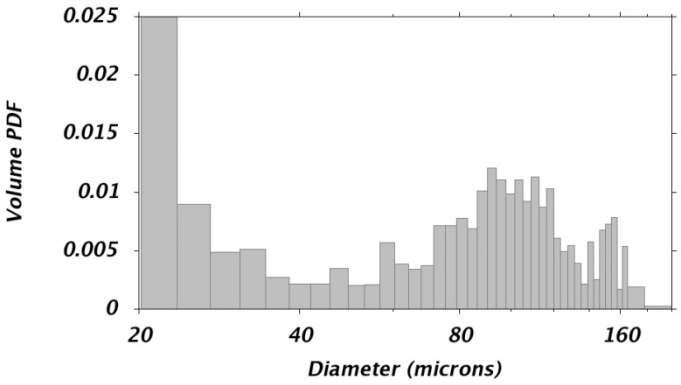

Figure 7: Obtained agglomerate size distribution

The size distribution we obtain is consistent with typical experimental results with a part of non-agglomerated particles (D=20µm) and a mean D_{43} diameter between 90µm (100µm if non-agglomerated particles are omitted in the calculation). Agglomerate size given by classical approaches is listed in Table 1:

Table 1: Agglomerate size predicted by classical approaches on studied propellant

	Beackstead [2]	**Salita [1]**	**Cohen [3]**
Mean agglomerate size (µm)	61	147	121

From a qualitative standpoint the result of our model is consistent with the above values. The fact that we obtain very large variations in the agglomerate sizes with classical approaches clearly legitimates the development of more evolved models such as the one presented in this paper as they could yield more accurate and detailed information about agglomeration.

7. Conclusion and perspectives

This paper introduces a phenomenological model for prediction of aluminum agglomeration. The methodology is based on a weak coupling with a mesoscale code dedicated to the simulation of solid propellant combustion. Conditions at and above the surface are extracted from the combustion code and used as input data for a phenomenological agglomeration model. Explicit tracking of aluminum particles enables us to track formation of aggregates at the surface, their mobility and transformation into agglomerates under thermal and aerodynamic stress. Preliminary application of the methodology on a typical industrial propellant shows encouraging results and predicts an agglomerate size distribution qualitatively consistent with classical approaches. Further studies will now focus on the impact of the free parameters of the model that mostly drive surface mobility and aerodynamic ejection of non-coalesced aggregates into the flow and on the impact of pressure on agglomeration. Comparison with experimental data will also be addressed.

Acknowledgments

This work was funded by the French Defense Procurement Agency (DGA).

References

[1] E.W.Price, K.J.Kraeutle, J.L.Prentice, T.L.Boggs, J.E.Crump and D.E.Zurn. 1982. Behavior of aluminum in solid propellant combustion. In: *NWC Report NWCTP6120*.

[2] M. Salita. 1994. Survey of recent Al2O3 droplet size data in solid rocket chambers, nozzles and plumes. In: *31st JANNAF Combustion Meeting.*

[3] M.W. Beckstead. 1977. A model for solid propellant combustion. In: *14th JANNAF Combustion Meeting.*

[4] N.S. Cohen. 1983. A pocket model for agglomeration in composite propellants. *AIAA J*. 21(5):720-725.

[5] V.Grigoriev, K.Kutsenogii and V.Zarko. 1981. Model of aluminum agglomeration during the combustion of composite propellant. *Comb. Explo. Shock Waves.* 17:354-362.

DOI: 10.13009/EUCASS2017-148

[6] V.A.Babuk, V.A.Vasil'ev and V.V.Sviridov. 1999. Modeling the structure of composite solid rocket fuel. *Comb. Explo. Shock Waves.* 35:144-148
[7] S.A.Rashkovskii. 1999. Structure of heterogeneous condensed mixtures. *Comb. Expl. Shock Waves.* 35:523-531.
[8] S.Gallier. 2009. A stochastic pocket model for aluminum agglomeration in solid propellants. *Propellants Explos. Pyrotech.* 34:97-105.
[9] A.Bandera, F.Maggi and L.T.De Luca. 2009. Agglomeration of aluminized solid rocket propellants. In: *Proc. of 45th AIAA/ASME/SAE/ASEE Joint Propulsion Conference & Exhibit.* 5439.
[10] T.Jackson, F.Najar and J.Buckmaster. 2005. A new class of agglomeration models for aluminized composite propellants based on random packs. *J. Prop. Power.* 21:925-936.
[11] O.B.Kovalev. 2002. Motor and plume particle size prediction in solid-propellant rocket motors. *J. Prop. Power.* 18:1199-1210.
[12] J.K.Sambamurthi, E.W.Price and P.K.Sigman. 1984. Aluminium agglomeration in solid-propellant combustion. *AIAA J.* 22:1132-1138.
[13] A.Gany and L.H.Caverny. 1979. Agglomeration and ignition mechanism of aluminum particles in solid propellants. In: *Symposium (International) on Combustion.* 17:1453-1461.
[14] Y.Yavor and A.Gany. 2008. Effet of nickel coating on aluminum combustion and agglomeration in solid propellants. In: *Proc. of 44th AIAA/ASME/SAE/ASEE Joint Propulsion Conference & Exhibit.* 5255.
[15] V.Srinivas and S.R.Chakravarthy. 2007. Computer model of aluminum agglomeration on burning surface of composite solid propellant. *J. Prop. Power.* 23:7238-736.
[16] K.Sankaralingam and S.R.Chakravarthy. 2000. A computer model of flamelet distribution on the burning surface of a composite solid propellant. *Combust. Sci. Tech*. 161:49-68.
[17] S.A.Rashkovskii. 2005. Statistical simulation of aluminum agglomeration during combustion of heterogeneous condensed mixtures. *Comb. Expl. Shock Waves.* 41:174-184.
[18] M.W.Beckstead, R.L.Derr, C.F.Price. 1970. A model of composite solid propellant combustion based on multiple flames, *AIAA J.* 8:2200-2207.
[19] S.Gallier, A.Ferrand, M.Plaud. 2016. Three-dimensional simulations of ignition of composite solid propellants. *Combust. Flame.* 173:2-15.
[20] E.W.Price, S.R.Chakravarthy, J.K.Sambamurthi and S.K.Sigman. 1998. The details of combustion of ammonium perchlorate propellants: Leading Edge Flame Detachment. *Combust. Sci. Tech*. 138:63-83.